An Analysis of Wave–Turbulence Interaction

D. FUA

Cooperative Institute for Research in Environmental Sciences (CIRES), University of Colorado/NOAA, Boulder 80309 and IFA/CNR, 00044 Frascati, Italy

G. CHIMONAS AND F. EINAUDI

School of Geophysical Sciences, Georgia Institute of Technology, Atlanta 30332

O. ZEMAN

Chesapeake Bay Institute and The Earth and Planetary Science Department, The Johns Hopkins University, Baltimore, MD 21218

(Manuscript received 18 January 1982, in final form 28 June 1982)

ABSTRACT

We present the results of an analytical and numerical calculation of the interaction between an internal gravity wave and a wave-induced turbulence. The initial atmospheric state, assumed horizontally homogeneous, is statically and dynamically stable with the background Richardson number Ri_0 approaching ¼ over some height regions. An initial non-singular neutral gravity wave propagates through such a system and modifies the Richardson number. The new Richardson number Ri may become smaller than ¼ and turbulence may develop. Using a "1½th order" scheme for the turbulence, we calculate the mean and the fluctuating part of the eddy diffusion coefficient. We show that the fluctuating part of the diffusion coefficient, because of its amplitude and phase, may overcome the damping effect of its mean part and force the original wave to grow in time. As the wave grows, it may further lower the Richardson number, increase the intensity of the turbulence, and further strengthen its interaction with it. At least in its initial stages, wave-induced turbulence appears to be an effective mechanism for transfer of energy from the background state into the wave. By showing that the early stages of the wave-induced turbulence interaction can lead to energy being transferred into the wave, we strengthen the case for gravity waves as important elements in the generation of turbulence in the atmosphere. The values we obtain for the eddy diffusion coefficients suggest that the process is quite capable of producing the empirically observed mixing rates at substantial heights above the ground. While the present calculations cannot describe the long-time limit of the wave–turbulence system, one may suggest that the often observed atmospheric conditions in which turbulence and waves appear to co-exist for several hours may result from a sort of equilibrium between the roles of the mean and the fluctuating parts of the eddy diffusion coefficient in taking away from and feeding energy into the wave.

1. Introduction

The interaction between gravity waves and turbulence has been invoked extensively to explain a variety of phenomena in the ocean and the atmosphere. The structure of the thermocline, the narrow layers of intense turbulence observed in the atmosphere, and the intermittent nature and patchiness of small-scale and clear-air turbulence have all been related to some form of wave-turbulence interaction.

The wave–turbulence system is complex because of the nonlinearities involved and the various energy exchanges which can occur among its components. In the theoretical treatment of geophysical flows, one often resorts to separating mean (background), periodic (wave), and random turbulent motions. Although, in general, these three motions interact strongly and are therefore inseparable, several flows appear to be dominated by the interactions between two of the components. For example, a daytime atmospheric boundary layer (ABL) is typically dominated by turbulence–mean flow interaction since an effective eddy viscosity is too large to allow waves of significant energy levels, at least for waves which owe their energy to a source within the ABL. However, flows above the boundary layer (above the first inversion) may be devoid of turbulence over some height ranges and mean flow–internal gravity wave interactions may be dominant.

Several authors have realized that a wave disturbance, acting within an otherwise stable background forms a system dominated by yet another interactive pair, i.e., the wave–turbulence coupling. They have proposed such coupling as the source of naturally occurring turbulence in the upper atmosphere (Hodges, 1967, 1969), in the ocean thermocline (Orlanski and Bryan, 1969; Phillips, 1980) and in the troposphere (Browning and Watkins, 1970; Browning

0022-4928/82/112450-14$07.50

et al., 1970; Gossard *et al.*, 1971; Van Zandt *et al.*, 1978).

The four basic ideas underlying the wave–turbulence coupling can be stated as follows:

1) The occurrence of turbulence can be related to the local (wave modified) Richardson number.
2) The turbulence occurs with a mean and a periodic component.
3) The turbulence extracts energy from the wave, limiting its growth, or feeds energy back into the wave.
4) The turbulence modifies the mean fields.

The first point is based on the working hypothesis that the stability of a time and space modulated flow, such as a gravity wave, is governed by the same criteria as a horizontally homogeneous, time independent background flow, provided the wave modified Richardson number is used. Such a hypothesis is corroborated by semi-quantitative arguments (Phillips, 1980) as well as by recently presented experimental evidence (Kondo *et al.*, 1978). The second point is related to the first and some experimental evidence for its validity has been recently obtained (Finnigan and Einaudi, 1981). The extraction of energy from the wave results from the mean component of the turbulence, while the periodic component, acting on the mean fields of the system, will generate a wave-like forcing term. The latter may, under certain circumstances, sufficiently reinforce the basic wave to overcome the effect of the mean component of the turbulence, leading to an overall wave–turbulence growth at the expense of the mean field energy (Chimonas, 1972).

In this paper, we investigate the problem of turbulence–gravity wave interaction for a statically stable atmosphere in which the background Richardson number Ri_0 is slightly larger than ¼ over some height regions. In these regions, a neutral gravity wave propagating through the system modifies the Richardson number and lowers it below ¼. As soon as this occurs, we assume that turbulence begins to form and we study its evolution in time and its interaction with the wave. The turbulence is parameterized by a so-called "1½th order" scheme in which the equation providing the evolution of the eddy diffusion coefficient $K \propto v$, ($v^2 = \frac{1}{2}\langle u_i' u_i' \rangle$ u_i' being the ith component of turbulence velocity), is derived from the equation for the turbulence kinetic energy. This scheme, although not as rigorous as a second order one (Deardorff, 1973, 1974), allows us to calculate the mean and the fluctuating part of the eddy diffusion coefficients, $\bar{K}$ and $\tilde{K}$, respectively. It is the presence of a perturbation in the eddy viscosity coefficients that creates the possibility for a constructive interaction between the wave and the wave-induced turbulence, the mean part $\bar{K}$ being responsible for damping of wave energy.

It should perhaps be emphasized that we are treating here an initially monochromatic disturbance and not a background spectrum of internal gravity waves leading to various forms of weak and strong nonlinear interactions (Phillips, 1980; Orlanski and Cerasoli, 1981).

In Section 2 we derive the equation of motion and we discuss the parameterization of the turbulence. In Section 3 an analytical solution is presented, together with some approximations appropriate to the problem at hand. Section 4 illustrates the numerical results.

2. The equations of motion and the parameterization of the turbulence

The equations of motion for an inviscid fluid can be written as (Lumley and Panofsky, 1964):

$$\rho \frac{d}{dt} u_i = -\frac{\partial p}{\partial x_i} - \rho g \delta_{i3}, \tag{2.1}$$

$$\frac{d}{dt}\rho + \rho \frac{\partial u_i}{\partial x_i} = 0, \tag{2.2}$$

$$\frac{d}{dt}\Theta = 0, \tag{2.3}$$

where ρ, p, Θ and u_i are the density, pressure, potential temperature and velocity of the fluid; g is the acceleration of gravity; δ_{ij} is the Kronecker delta and the x_3-axis is taken vertically upward. We also adopt the Einstein summation convention. The above are the equations for conservation of momentum, mass and energy, respectively, with the substantial time derivative given by

$$\frac{d}{dt} = \frac{\partial}{\partial t} + u_i \frac{\partial}{\partial x_i}. \tag{2.4}$$

The Coriolis force has been neglected because of the relatively small spatial and temporal scales of the disturbances we will analyze; molecular viscosity and heat conduction have been neglected on the working assumption that the wave-induced turbulence will be a dominating element.

We now adopt a triple decomposition whereby each variable $b(t, x_i)$ is decomposed as the sum of a mean part $\bar{b}$, a periodic component $\tilde{b}$, and a turbulent component b':

$$b(t, x_i) = \bar{b}(x_i) + \tilde{b}(t, x_i) + b'(t, x_i). \tag{2.5}$$

Following Reynolds and Hussain (1972), we introduce a time and a phase average operator

$$\bar{b} = \lim_{t\to\infty} \frac{1}{2t} \int_{-t}^{t} b(t')dt', \tag{2.6}$$

$$\langle b \rangle = \bar{b} + \tilde{b} = \lim_{N\to\infty} \frac{1}{N} \sum_{n=1}^{N} b(t + n\tau), \tag{2.7}$$

where τ is the period of the wave. The first is the straightforward time average operator, while the second averages over a large ensemble of points having the same phase with respect to the known gravity wave which acts as a reference oscillator. It may often be advantageous to define the decomposition using space coordinates x_1 and x_2 rather than t. The reformulation of (2.6) *et seq.* is relatively straightforward. The spacelike average and selection are obligatory, if temporal evolution of the mean flow is considered.

Following the general approach of turbulence theory, we can derive a number of coupled equations from (2.1)–(2.3), by applying the time and phase average operators to them and performing a number of appropriate manipulations. Of particular interest to us here are the equations governing the organized wave:

$$\bar{\rho}\left[\frac{\partial \tilde{u}_i}{\partial t} + \bar{u}_j \frac{\partial}{\partial x_j}\tilde{u}_i + \tilde{u}_j \frac{\partial}{\partial x_j}\bar{u}_i\right] = -\frac{\partial \tilde{p}}{\partial x_i} - g\tilde{\rho}\delta_{i3} - \frac{\partial}{\partial x_j}\tilde{R}_{ij} - \frac{\partial}{\partial x_j}\tilde{r}_{ij}, \quad (2.8)$$

$$\frac{\partial}{\partial x_i}(\bar{\rho}\tilde{u}_i) = 0, \quad (2.9)$$

$$\bar{\rho}c_p\left[\frac{\partial}{\partial t}\tilde{\Theta} + \bar{u}_i\frac{\partial \tilde{\Theta}}{\partial x_i} + \tilde{u}_i\frac{\partial}{\partial x_i}\bar{\Theta}\right] = -\frac{\partial}{\partial x_i}[\tilde{E}_i + \tilde{e}_i], \quad (2.10)$$

where

$$\tilde{R}_{ij} = \bar{\rho}[\tilde{u}_j\tilde{u}_i - \widetilde{\bar{u}_j\bar{u}_i}], \quad \tilde{r}_{ij} = \bar{\rho}[\langle u'_j u'_i\rangle - \widetilde{\overline{u'_j u'_i}}], \quad (2.11)$$

$$\tilde{E}_i = c_p\bar{\rho}[\tilde{u}_i\tilde{\Theta} - \widetilde{\bar{u}_i\bar{\Theta}}],$$

$$\tilde{e}_i = c_p\,\bar{\rho}[\langle u'_i\Theta'\rangle - \widetilde{\overline{u'_i\Theta'}}]. \quad (2.12)$$

These equations are briefly derived in the Appendix, where a discussion of the approximations involved is also provided. The function $-\tilde{R}_{ij}$ represents the fluctuation part of the nonlinear wave contribution to the Reynolds stress, while $-\tilde{r}_{ij}$ can be viewed as the oscillating part of the background Reynolds stress due to the presence of the wave. Equivalently, $-\tilde{E}_i$ and $-\tilde{e}_i$ are related to the oscillating parts of the heat flux carried by the wave and the turbulent fluctuations, respectively.

Proceeding in a similar fashion, one can derive an equivalent set of equations for the turbulent fluctuations, the mean field quantities, the $\bar{r}_{ij}$'s and the $\bar{e}_i$'s. The equations for the $\bar{r}_{ij}$'s and the $\bar{e}_i$'s contain many terms which are not known, a manifestation of course of the closure problem characteristic of turbulent processes. To close the system we will have to make somewhat *ad hoc* assumptions concerning the behavior of the $\tilde{r}_{ij}$'s and the $\tilde{e}_i$'s.

Most of the turbulence models are based on the weak interaction assumption; i.e., turbulence is presumed to be statistically steady and to have characteristic time and spatial scales which are well separated from those of the mean flow and the wave motion. Although the spatial separation of scales is not entirely satisfied in boundary layers, the more sophisticated turbulence models, such as second-order closure models, predict the statistical properties of turbulence remarkably well. (For a review of turbulence models see Zeman, 1981.) In the present study it is necessary to model the generation of turbulence due to wave-induced instability. Turbulence is not necessarily in statistical equilibrium and due to extreme buoyancy forces it may, in reality, degenerate into some quasi-two dimensional motion, once the source of instability is removed. Little is known about the behavior of turbulence under such extreme conditions and therefore any model will only be able to reproduce within an order of magnitude, realistic spacial and temporal growth of turbulence. Fortunately, the results do not appear to be overly sensitive to the exact choice of model parameters.

The simplest closure scheme for the turbulent fluctuations is a constant eddy viscosity model (see Reynolds and Hussain, 1972, and references therein). The turbulence affects the wave through the mean velocity profile and not through the wave stresses. Thus, the $\tilde{r}_{ij}$'s are zero and the time average of $u'_i u'_j$ is expressed as

$$\left.\begin{aligned}\overline{u'_i u'_j} &= \tfrac{1}{3}\delta_{ij}\overline{u'_m u'_m} - \bar{K}\bar{\mathbf{S}}_{ij}\\ \bar{\mathbf{S}}_{ij} &= \left(\frac{\partial \bar{u}_i}{\partial x_j} + \frac{\partial \bar{u}_j}{\partial x_i}\right)\end{aligned}\right\}, \quad (2.13)$$

where $\bar{K}$ is a constant eddy viscosity and the strain rate tensor $\bar{\mathbf{S}}_{ij}$ involves background quantities only. The overall effect of the turbulence will usually be to subtract energy from the wave.

If, still within the context of a constant viscosity model, we allow the turbulence to affect the wave through the wave stresses as well, then the phase average of the quantity $u'_i u'_j$ can be expressed as

$$\left.\begin{aligned}\langle u'_i u'_j\rangle &= \tfrac{1}{3}\delta_{ij}\langle u'_m u'_m\rangle - \bar{K}\mathbf{S}_{ij}\\ \mathbf{S}_{ij} &= \bar{\mathbf{S}}_{ij} + \tilde{\mathbf{S}}_{ij}, \quad \tilde{\mathbf{S}}_{ij} = \left(\frac{\partial \tilde{u}_i}{\partial x_j} + \frac{\partial \tilde{u}_j}{\partial x_i}\right)\end{aligned}\right\}. \quad (2.14)$$

Although the wave stresses are now present in $\mathbf{S}_{ij}$, the turbulent stress remains in phase with the strain rate and it may be shown that such a coupling between turbulence and wave leads to wave energy dissipation.

If turbulence is to interact with a wave in a constructive way, perturbations of the eddy viscosity coefficient K by the wave itself have to be considered. We shall further make the working hypothesis that

the strain rate tensor $\mathbf{S}_{ij}$ will depend on the gradients of the gravity wave as well as of the background wind. Thus, we shall write:

$$K = \bar{K} + \tilde{K}, \quad \mathbf{S}_{ij} = \bar{\mathbf{S}}_{ij} + \tilde{\mathbf{S}}_{ij}, \tag{2.15}$$

with

$$\tilde{\mathbf{S}}_{ij} = (\partial \tilde{u}_i/\partial x_j + \partial \tilde{u}_j/\partial x_i). \tag{2.16}$$

Assuming that $u'_i u'_j$, K and $\bar{\mathbf{S}}_{ij}$ have the same formal relationship as in the constant K theory, we can write $\langle u'_i u'_j \rangle$, $\overline{u'_i u'_j}$ and $\tilde{r}_{ij}$ as follows:

$$\langle u'_i u'_j \rangle = \tfrac{1}{3}\langle u'_m u'_m \rangle \delta_{ij} - (\bar{K}\bar{\mathbf{S}}_{ij} + \tilde{K}\tilde{\mathbf{S}}_{ij} + \bar{K}\tilde{\mathbf{S}}_{ij} + \tilde{K}\bar{\mathbf{S}}_{ij}), \tag{2.17}$$

$$\overline{u'_i u'_j} = \tfrac{1}{3}\delta_{ij}\overline{u'_m u'_m} - (\bar{K}\bar{\mathbf{S}}_{ij} + \overline{\tilde{K}\tilde{\mathbf{S}}_{ij}}), \tag{2.18}$$

$$\tilde{r}_{ij} = \bar{\rho}\left\{\frac{\delta_{ij}}{3}(\langle u'_m u'_m \rangle - \overline{u'_m u'_m}) - [\bar{K}\tilde{\mathbf{S}}_{ij} + \tilde{K}\bar{\mathbf{S}}_{ij} + (\tilde{K}\tilde{\mathbf{S}}_{ij} - \overline{\tilde{K}\tilde{\mathbf{S}}_{ij}})]\right\}. \tag{2.19}$$

In (2.19) the functions $\tilde{\mathbf{S}}_{ij}$ and $\bar{\mathbf{S}}_{ij}$ should be considered known, once the background and wave fields are known. Proceeding similarly and adopting a relationship commonly used in turbulence theory (see Monin and Yaglom, 1971), we write:

$$\langle \Theta' u'_i \rangle = -\alpha_0(\bar{K} + \tilde{K})\frac{\partial}{\partial x_i}(\bar{\Theta} + \tilde{\Theta}), \tag{2.20}$$

$$\overline{\Theta' u'_i} = -\alpha_0\left[\bar{K}\frac{\partial}{\partial x_i}\bar{\Theta} + \overline{\tilde{K}\frac{\partial}{\partial x_i}\tilde{\Theta}}\right], \tag{2.21}$$

$$\tilde{e}_i = -c_p\bar{\rho}\alpha_0\left[\bar{K}\frac{\partial}{\partial x_i}\tilde{\Theta} + \tilde{K}\frac{\partial}{\partial x_i}\bar{\Theta} + \left(\tilde{K}\frac{\partial}{\partial x_i}\tilde{\Theta} - \overline{\tilde{K}\frac{\partial}{\partial x_i}\tilde{\Theta}}\right)\right], \tag{2.22}$$

where α_0, the ratio of the eddy diffusivities for temperature and momentum, will be considered a given time- and space-invariant. This assumption is, of course, highly hypothetical, especially in the present context of both diffusivities being dependent on time and spatial coordinates. To determine the $\tilde{r}_{ij}$'s and the $\tilde{e}_i$'s we still have to find K. The equation for K will be derived from the turbulent kinetic energy equation and the constitutive relations for K and the rate of turbulent energy dissipation ϵ_d in terms of the turbulent kinetic energy itself and the length scale l of turbulence.

The equation for the turbulent kinetic energy, derived in the Appendix, can be written as

$$\left.\begin{aligned}\frac{dv^2}{dt} &= -\frac{2}{3}v^2\frac{\partial}{\partial x_j}(\bar{u}_j + \tilde{u}_j) \\ &+ K\mathbf{S}_{ij}\frac{\partial}{\partial x_j}(\bar{u}_i + \tilde{u}_i) \\ &\times\left[1 + \frac{g}{\bar{\Theta} + \tilde{\Theta}}\frac{\langle u'_3\Theta'\rangle}{K\mathbf{S}_{ij}\dfrac{\partial}{\partial x_j}(\bar{u}_i + \tilde{u}_i)}\right] - \epsilon_d\end{aligned}\right\}, \tag{2.23}$$

where

$$v^2 = \tfrac{1}{2}\langle u'_i u'_i \rangle, \quad \frac{d}{dt} = \frac{\partial}{\partial t} + (\bar{u}_j + \tilde{u}_j)\frac{\partial}{\partial x_j}. \tag{2.24}$$

For the cases we will consider in this paper, it is a good approximation to write

$$\mathbf{S}_{ij}\frac{\partial}{\partial x_j}(\bar{u}_i + \tilde{u}_i) \approx \left(\frac{\partial \bar{u}_1}{\partial x_3} + \frac{\partial \tilde{u}_1}{\partial x_3}\right)^2. \tag{2.25}$$

If we define a modified Richardson number in which the wave terms are included as

$$\mathrm{Ri} = \frac{g}{\bar{\Theta} + \tilde{\Theta}}\frac{\partial}{\partial x_3}(\bar{\Theta} + \tilde{\Theta})\left[\frac{\partial}{\partial x_3}(\bar{u}_1 + \tilde{u}_1)\right]^{-2}, \tag{2.26}$$

we can cast (2.23) in the form

$$\frac{dv^2}{dt} = -\frac{2}{3}v^2\frac{\partial}{\partial x_j}(\bar{u}_j + \tilde{u}_j) + K\left(\frac{\partial \bar{u}_1}{\partial x_3} + \frac{\partial \tilde{u}_1}{\partial x_3}\right)^2[1 - \alpha_0\,\mathrm{Ri}] - \epsilon_d. \tag{2.27}$$

In analogy with molecular transport, K has to depend on some characteristic velocity v and length scale l of the turbulence:

$$K = \alpha_K v l, \tag{2.28}$$

where α_K is a numerical constant. Information on the magnitude of v is contained in (2.27). In boundary layers it is customary to use Prandtl's mixing length hypothesis and l is set proportional to the distance x_3 from the ground. In more complex flows, $l \sim x_3$ may not be a relevant length scale and a dissipation equation may be employed instead (Zeman and Lumley, 1976).

The length scale l and the dissipation rate ϵ_d are related by the empirical law (Batchelor, 1953),

$$\epsilon_d = \alpha_\epsilon v^3/l, \tag{2.29}$$

α_ϵ being an empirical constant.

In our flow, the situation is somewhat unorthodox. Both ϵ_d and v may be initially zero and the empirical law (2.29) is then physically meaningless; needless to say, the scales of turbulence are unrelated to the distance from the ground. It makes sense to postulate that the length scale is related to the vertical size Λ

of the region of wave-induced instability. The scale of the largest eddies is expected to be proportional to the vertical extent of the region where the modified Richardson number, given by (2.26), decreases below the critical value 1/4. As mentioned earlier, our system is statically stable, with values of the Richardson number slightly above 1/4 over some height ranges. A finite amplitude gravity wave, passing through such a system, may give rise to one or more isolated regions where the wave-modulated Richardson number is <1.4. Such regions will have a vertical size which increases with the wave amplitude and will have a tendency to be elongated horizontally, since the waves will have horizontal wavelengths much larger than the vertical ones and the wave amplitude, although finite, will be chosen to be "small."

Since the phase velocity of the wave is, in general, different from the background wind speed (we are not considering here cases with a critical level), the turbulent patches will find themselves alternatively in regions where Ri is less or larger than 1/4. The turbulence, because of relaxation effects, will not disappear as soon as Ri becomes >1/4: in such regions the turbulence length scale l will be chosen equal to

$$\Lambda_0 = v/n, \tag{2.30}$$

n being the Brunt-Väisälä frequency. This constraint on the turbulence length scale has been used by a number of authors (Brost and Wyngaard, 1978; Yamada and Mellor, 1979) and it simply implies that the turbulence potential energy (l^2n^2) cannot exceed its initial kinetic energy. In the cases we have analyzed, the contributions from these regions are not very important.

Using (2.28), (2.29) and the above definition of l, we can rewrite (2.27) as

$$\frac{d}{dt}\kappa = -\frac{\kappa}{3}\frac{\partial}{\partial x_j}(\bar{u}_j + \tilde{u}_j) + \frac{l}{2}\alpha_K{}^2\left[\frac{\partial}{\partial x_3}(\bar{u}_1 + \tilde{u}_1)\right]^2 \times (1 - \alpha_0 \mathrm{Ri}) - \frac{\alpha_\epsilon}{\alpha_K}\frac{\kappa^2}{2l}, \tag{2.31}$$

where

$$\kappa = K/l. \tag{2.32}$$

At any given time and point in space, l will be determined as a function of the wave and background fields: κ and therefore K will be obtained from (2.31).

3. An analytical solution

We treat our problem as an initial value one, in which, at $t = 0$, a neutral gravity wave of known properties propagates through an atmosphere of given background parameters. The background Richardson number Ri_0 is larger than 1/4 everywhere and, over some height range, is given by

$$\mathrm{Ri}_0 = \tfrac{1}{4} + \delta, \quad \delta \ll 1. \tag{3.1}$$

No turbulence is assumed to exist for $t < 0$.

The formal analytical solution of the problem is obtained by first taking the Fourier transform in space and the Laplace transform in time of the original set of equations (2.8)–(2.10), and then solving the ensuing second-order differential equation by the Green's function technique. Here, we will define only the essential quantities and we will refer the reader to the paper by Chimonas *et al* (1980) for details about this kind of approach.

The Fourier transform in space and the Laplace transform in time of a quantity $a(x, z, t)$ are defined as:

$$a_k(k, z, t) = [a(x, z, t)] = \frac{1}{\sqrt{2\pi}}\int_{-\infty}^{\infty} a e^{ikx} dx, \tag{3.2}$$

$$\hat{a}(x, z, \omega) = [a(x, z, t)] = \frac{1}{\sqrt{2\pi}}\int_0^{\infty} a(x, z, t) e^{-\omega t} dt. \tag{3.3}$$

Our treatment assumes that the system is uniform in the $y = x_2$ coordinate. Note that $x \equiv x_1$ and $z = x_3$. It is convenient to introduce the new variable q which is essentially the vertical displacement of the wave:

$$\hat{q}_k = -\frac{\hat{w}_k}{i\Omega\epsilon_0}, \quad w = \tilde{u}_3, \tag{3.4}$$

$$\Omega = k\bar{u}_1 + i\omega, \quad \epsilon_0 = \exp\left[g\int\frac{dz}{C^2}\right], \tag{3.5}$$

$$C^2 = \gamma\bar{p}/\bar{\rho}, \quad \gamma = c_p/c_v, \tag{3.6}$$

c_p and c_v being the specific heats at constant pressure and volume, respectively. In terms of $\hat{q}_k$, the system of equations one obtains by taking the Fourier and Laplace transforms of (2.8)–(2.10), reduces to the equation

$$L(\hat{q}_k) = \hat{F}_k + I_0, \tag{3.7}$$

where the operator L is defined as

$$L = f\frac{d^2}{dz^2} + \frac{df}{dz}\frac{d}{dz} + k^2 r(n^2 - \Omega^2), \tag{3.8}$$

with

$$\left.\begin{aligned} f &= r\Omega^2, \quad r = \bar{\rho}\epsilon_0^2 \\ n^2 &= \frac{g}{\bar{\Theta}}\frac{d\bar{\Theta}}{dz}, \quad R = c_p - c_v \end{aligned}\right\}. \tag{3.9}$$

I_0 is a function of the values of the field variables at $t = 0$. The function $\hat{F}_k$ is given by

$$\hat{F}_k = k^2\epsilon_0\hat{Z}_k - \frac{\epsilon_0 g k^2}{i\Omega C^2}\hat{E}_k + \frac{d}{dz}\left[\frac{i\epsilon_0\Omega}{C^2}\left(\hat{E}_k - \frac{C^2 k}{\Omega}\hat{X}_k\right)\right], \tag{3.10}$$

where

$$X = -\frac{\partial}{\partial x_j}\tilde{r}_{1j}, \quad Z = -\frac{\partial}{\partial x_j}\tilde{r}_{3j}, \qquad (3.11)$$

$$E = -\frac{\gamma R}{c_p}\frac{\partial}{\partial x_j}\tilde{e}_j .$$

A number of approximations have been utilized in deriving (3.7), which are consistent with the validity of (2.9) and the assumption that $|\omega/kC|^2 \ll 1$. We have assumed $\bar{u}_2 = \bar{u}_3 = 0$ and we have neglected the contribution from the nonlinear terms $\tilde{R}_{ij}$ and $\tilde{E}_i$. Also not included is any coupling of the system with the y-component of the wave and the turbulence fields. The boundary conditions associated with (3.7) are

$$\hat{q}_k(0) = 0, \quad \text{and either} \quad \hat{q}_k(z \to \infty) = 0 \qquad (3.12)$$

or the radiation condition as $z \to \infty$, whichever is appropriate.

Formally treating $\tilde{F}_k$ and I_o as a forcing function for the wave field $\hat{q}_k$, we can write the solution of (3.7) as (see Courant and Hilbert, 1953, Sec. 14, Chap. 5; Chimonas *et al.*, 1980):

$$\hat{q}_k = -\int_0^\infty d\zeta G(\zeta, z)[\hat{F}_k(\zeta) + I_0(\zeta)], \qquad (3.13)$$

where $G(\zeta, z)$ is the Green's function defined as

$$G(\zeta, z) = \begin{cases} -\hat{q}_k^{(+)}(\zeta)\hat{q}_k^{(-)}(z)/d, & z \leqslant \zeta \\ -\hat{q}_k^{(-)}(\zeta)\hat{q}_k^{(+)}(z)/d, & z > \zeta \end{cases} \qquad (3.14)$$

and

$$d(k, \omega) = \left(\hat{q}_k^{(-)}\frac{\partial \hat{q}_k^{(+)}}{\partial z} - \hat{q}_k^{(+)}\frac{\partial \hat{q}_k^{(-)}}{\partial z}\right)f \qquad (3.15)$$

is independent of z. The functions $\hat{q}_k^{(+)}$ and $\hat{q}_k^{(-)}$ are the solutions of $L(\hat{q}_k) = 0$ obeying the upper and lower boundary conditions (3.12), respectively.

The inverse Laplace transform of $\hat{q}_k$ can be written as

$$q_k(k, z, t) = -\frac{1}{2\pi i}\int_{-i\infty+\gamma_0}^{i\infty+\gamma_0} d\omega e^{\omega t}\int_0^\infty d\zeta G(\zeta, z) \times [\hat{F}_k(\zeta) + I_0(\zeta)] = q_k^{(1)} + q_k^{(0)}, \qquad (3.16)$$

where $q_k^{(0)}$ is the value of q_k for $t < 0$, when no turbulence is assumed to occur. In general it is possible to write

$$G(\zeta, z)\hat{F}_k(\zeta) = \hat{g}_k(\zeta, z)\hat{s}_k(\zeta), \qquad (3.17)$$

where $\hat{s}_k$ is the Laplace and Fourier transform of a function $s(x, z, t)$ which includes all of the terms which depend on the turbulence. Using the convolution theorem (see Morse and Feshbach, 1953, Part 1, Chap. 4), $q_k^{(1)}$ can be written as

$$q_k^{(1)}(k, z, t) = -\int_0^\infty d\zeta \int_0^t g_k(t - \tau, z, \zeta)s_k(\tau, \zeta)d\tau. \qquad (3.18)$$

By taking the inverse Fourier transform of (3.16) and using (3.18) we obtain the expression for $q(x, z, t)$:

$$q(x, z, t) = q^{(0)}(x, z, t) + q^{(1)}(x, z, t) = q^{(0)}(x, z, t) + (2\pi)^{-1/2}\int q_k^{(1)}(k, z, t)e^{-ikx}dk. \qquad (3.19)$$

Eq. (3.19) is the formal solution for the initial system (2.8)–(2.10). It is an implicit solution since $q^{(1)}$ depends on q through the turbulence terms.

There are two kinds of approximations we now introduce: one consists of an approximate representation for s_k and hence for the turbulent terms. The second consists of an approximate calculation of g_k. We outline briefly the reasoning for these approximations.

Eq. (2.31) is solved using a leap-frog method. It provides the value of K at $t = t_{n+2}$ once the value of K is known at $t = t_n$ and the values of the background quantities, the wave fields and of l are determined at $t = t_{n+1}$. Having found $K(t_{n+2}, x, z)$ we then proceed to calculate the wave variables at $t = t_{n+3}$ and so on. For given t and z we can calculate the Fourier series representation for K. Such an expansion will depend on the background system and on the initial wave. We assume an initial monochromatic wave with horizontal wavenumber k_0 and frequency ω_0 which we can represent as

$$q_0(x, z, t) = A_0\hat{q}_{k_0}\exp(\omega_0 t - ik_0 x), \qquad (3.20)$$

where A_0 is an amplitude factor chosen to induce turbulence at $t = 0$. The induced turbulence is expected to have some sort of periodic structure in the x direction and we will represent K as

$$K(x, z, t) = \sum_n K^{(n)}(z, t)\exp(-ink_0 x), \qquad (3.21)$$

with a corresponding Fourier transform given by

$$K_k(k, z, t) = (2\pi)^{1/2}\sum_n K^{(n)}\delta(k - nk_0), \qquad (3.22)$$

where δ is the Dirac delta function. In the calculations, we have neglected all terms with wavenumber higher than k_0, on the assumption that they are small compared with the fundamental and that they do not contribute, to first order, to the feedback of the turbulence on the initial wave. It follows that X, Z and E, defined by (3.11), will be represented simply by

$$X = X_{(0)} + X^{(1)}, \quad Z = Z_{(0)} + Z^{(1)}, \quad E = E_{(0)} + E^{(1)}, \qquad (3.23)$$

where suffixes 0 and 1 refer to the mean values and the first components, respectively.

The evaluation of g_k requires the integration in the complex ω-plane of $\hat{g}_k$. In calculating g_k, we have made the conventional assumption that the dynamics of the system is dominated by the modes of the mean atmosphere, so that g_k can be written as

$$g_k(k, z, t) = \frac{1}{2\pi i}\int_{-i\infty+\gamma_0}^{i\infty+\gamma_0} \hat{g}_k(k, z, \omega)e^{\omega t}d\omega \approx \sum_j \text{(residues at } \omega_j). \quad (3.24)$$

Because of the nature of the initial wave, we will have the contribution from ω_0 only.

Because of the above assumptions, the final result will read

$$q(x, z, t) \approx \tilde{q}_{k_0}A_0[\exp(\omega_0 t - ik_0 x)][1 + A(t)], \quad (3.25)$$

with

$$A(t) = -\int_0^t d\tau \frac{\exp(-\omega_0\tau)}{f(0)\left[\frac{\partial\hat{q}_k}{\partial z}\cdot\frac{\partial\hat{q}_k}{\partial\omega}\right]_{k_0,\omega_0}}\int_0^\infty d\zeta\epsilon_0$$

$$\times\left\{k_0^2\hat{q}_{k_0}(\zeta)\left[Z^{(1)}(\zeta, \tau) + i\frac{E^{(1)}(\zeta, \tau)}{\Omega_0}\frac{1}{\epsilon_0}\frac{d\epsilon_0}{d\zeta}\right]\right.$$

$$\left. + ik_0\frac{\partial\hat{q}_{k_0}}{\partial\zeta}\left[X^{(1)}(\zeta, \tau) - k_0\frac{E^{(1)}(\zeta, \tau)}{\Omega_0}\frac{\Omega_0^2}{C^2k_0^2}\right]\right\}, \quad (3.26)$$

with

$$\Omega_0 = k_0\bar{u}_1 + i\omega. \quad (3.27)$$

Eq. (3.25) is the final analytical result which we utilize in the numerical calculations. The nature of the feedback between the wave-induced turbulence and the wave itself will depend on the behavior of $A(t)$.

4. Numerical results

The objective of the calculations is to evaluate $A(t)$ given by (3.26). If the amplitude and phase of $A(t)$ are such that $|1 + A(t)|$ decreases with time, then the feedback is negative, the initially neutral gravity wave will decay in time, and the induced turbulence will most likely cease to exist. If, however, $|1 + A(t)|$ increases with time, then the gravity wave may further modify the Richardson number, the wave-induced turbulence may increase, and the overall system may be quite different from the initial one. Our treatment can describe the early stages of triggering of, and interaction with, turbulence, when such an interaction is relatively weak. We cannot follow the system to later stages, when the interaction will be highly nonlinear.

The calculations proceed in three stages: 1) the calculations of the neutral modes of the background atmosphere; 2) the analysis of the turbulence structure at a given time; 3) the calculation of $A(t)$ given by (3.26).

a. Determination of the Green's function

To construct the Green's function G, defined by (3.14), we need to determine the solutions of

$$L(\hat{q}_k) = 0,$$

i.e., the values of wavenumbers k_0 and frequency ω_0, such that the corresponding eigenfunctions $\hat{q}_k$ satisfy the appropriate boundary conditions. The knowledge of k_0, ω_0 and $\hat{q}_k$ defines completely the initial gravity wave propagating in the assigned background. We consider two separate background states. Model 1 is the often-used case where the Brunt-Väisälä frequency square and the normalized background wind are both tangent hyperbolic functions of normalized height y. Model 2 is characterized by a low level jet in the presence of an elevated temperature inversion. The two models are represented in Figs. 1a and b, respectively. The common feature of the two models is the presence of relatively small regions in which the background Richardson number Ri_0 is slightly above 1/4, as described in Fig. 1. Thus, the background initial state is statically stable throughout and no turbulence is present: over those regions where Ri_0 is slightly larger than 1/4, the gravity wave, small but finite, may lower Ri_0 below 1/4.

The normalized eigenvalues [$\alpha = kh$, $c_r = \omega/(kV)$], h and V being the characteristic length and velocity, respectively, are given in Fig. 2 for Model 1 and Fig. 6 for Model 2. The plotted curves are only some of all the possible families of nonsingular neutral modes [$\mathrm{Im}(\omega) = 0$ and no critical level] that each background state can support.

Examples of the corresponding eigenfunctions are given in Fig. 3 for Model 1 and Fig. 7 for Model 2. In these figures, the actual vertical displacements $\xi = A_0\tilde{q}_{k_0}$ [see Eq. (3.25)] are given as a function of height. Although there are no critical levels, the maximum amplitudes are reached where u_0 is closest to the value of the horizontal phase velocity. In all cases, the maximum vertical displacements of the initial wave are rather small ($< \sim 50$ m) to ensure that the initial linearization is valid. The amplitude of the initial gravity wave is chosen to lower the Richardson number below 1/4 and induce turbulence over a height range of no more than a few tens of meters. The precise value of such initial amplitude did not affect the nature of the feedback.

b. Analysis of the wave-induced turbulence

We have already discussed the constitutive relations for the treatment of turbulence in the previous

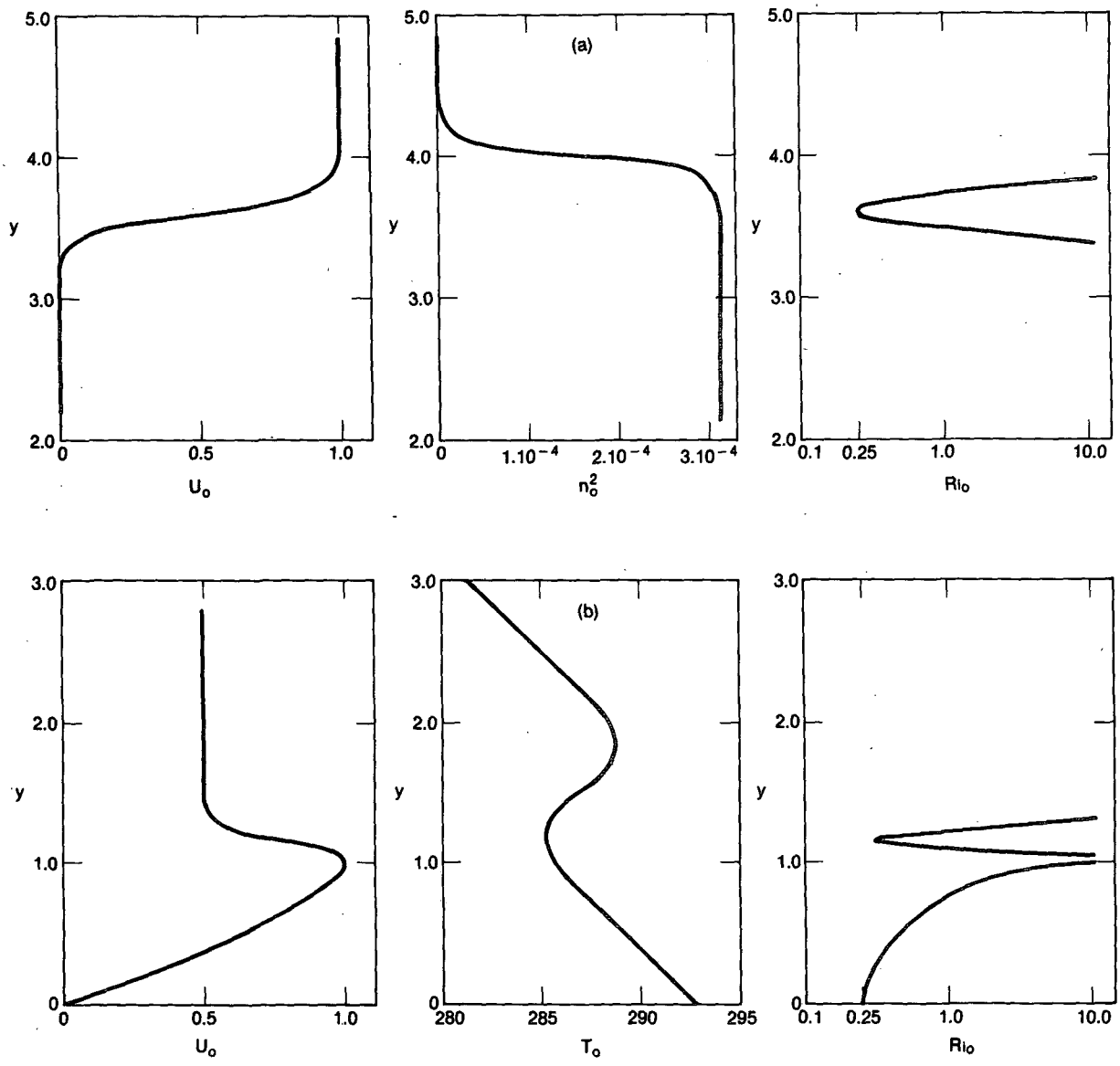

FIG. 1. (a) Model 1. Profiles of normalized horizontal background wind $u_0 = \bar{u}_1/V$ ($V = 5$ m s^{-1}), Brunt-Väisälä frequency square n_0^2 (s^{-2}) and background Richardson number Ri_0 as a function of normalized height $y = z/h$, with $h = 500$ m. (b) Model 2. As in (a), except that the background temperature T_0 (K) is plotted instead of n_0^2. T_0 tends to the asymptotic value of 250 K at $y = 10$. For this model $V = 10$ m s^{-1} and $h = 900$ m.

two sections. From the knowledge of the background and wave fields, we determine the modified Richardson number Ri, the length l, and the coefficients of (2.31): for given z and t, we then determine κ and hence K as a function of x and we calculate their Fourier representation. In the present approximation, we only need the mean and first harmonic of such an expansion, K_0 and K_1. It should be noted that at $t = 0$, κ is zero and that for the initiation of turbulence we need a value of $\mathrm{Ri} < 1/\alpha_0$. The values of the constants used in solving (2.31) are $\alpha_K = \alpha_\epsilon = 1$ and $\alpha_0 = 4$. Using values of α_k, α_ϵ and α_0 in the above neighborhood, we have not noticed appreciable changes in our results. Once K_0 and K_1 are known, X_1, Z_1, and E_1 are calculated and all the elements to evaluate (3.26) are thus available.

c. *The behavior of A(t)*

The final calculation of $A(t)$ is a straightforward integration in height and time. This completes a self-consistent treatment in which the mutual interaction of the wave and the turbulence is followed at each time step. At each value of time, the areas in space

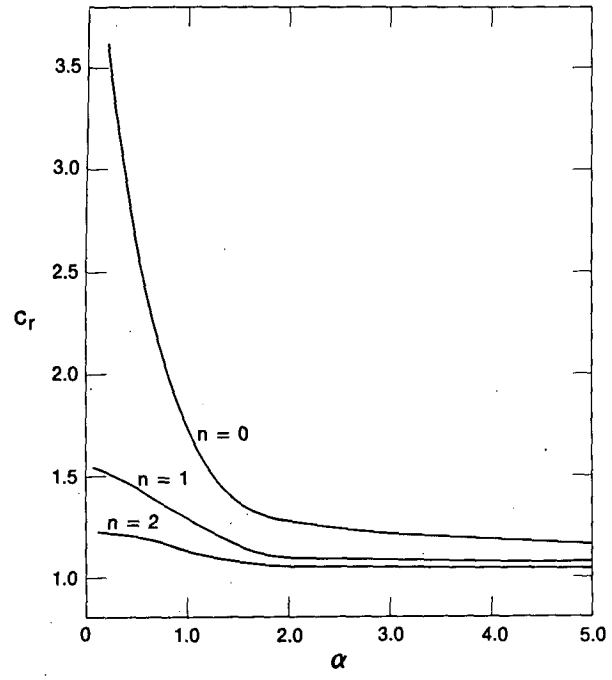

FIG. 2. Dispersion curves corresponding to nonsingular neutral modes of Model 1: c_r (horizontal phase velocity normalized with respect to $V = 5$ m s^{-1}) versus $\alpha = kh$, $h = 500$ m.

where Ri is less than 1/4 and K is different from zero can be mapped. Such areas provide qualitative information about the distribution of wave-induced turbulence and its evolution. Fig. 4 describes this evolution for a wave of Model 1 described by a normalized horizontal wavenumber $\alpha = 2$ and mode $n = 1$. The horizontal scale is the horizontal coordinate, normalized with respect to h, as measured in a frame of reference moving with the horizontal phase velocity of the wave. One can compare, for example, the region where K is different from zero at normalized time $\tilde{t} = 0.1$ (real time $t = 10$ s), with that at $\tilde{t} = 5$ ($t = 500$ s). It should not be surprising that the region where $K \neq 0$ increases much more rapidly than that where Ri $< \frac{1}{4}$: this is due to the diffusive nature of Eq. (2.31) which governs the evolution of K and the fact, mentioned earlier, that the phase velocity of the wave in both models is larger than the background wind. Also worth noticing is the elongated shape of such regions which, after a while, are essentially continuous in the horizontal direction. This situation provides support to the idea that the thin layers of turbulence often observed in the ocean and the earth's atmosphere are due to the presence of gravity waves. The number and characteristics of these layers will depend on the background state and the waves it will support.

It is perhaps important to point out that the region where Ri is less than $\frac{1}{4}$, is divided into two parts with a subregion where Ri becomes negative. This subregion only appears after some time t has evolved, and is the result of the wave increasing its amplitude and further modifying the initial Richardson number.

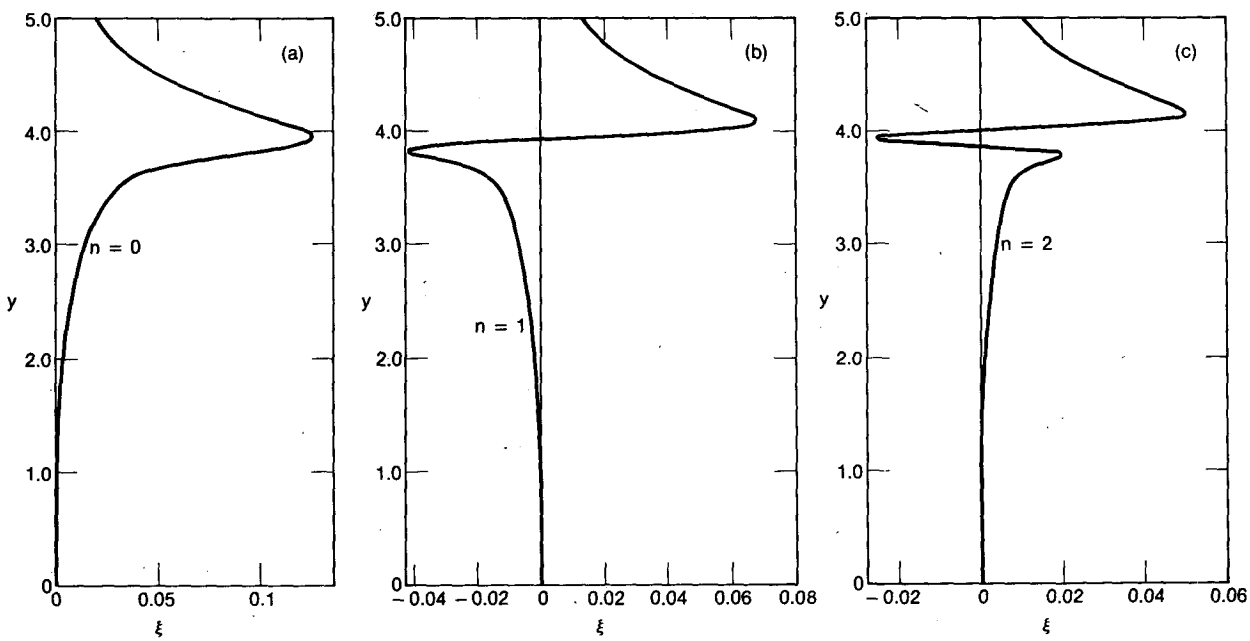

FIG. 3. Vertical displacements normalized with respect to $h = 500$ m versus $y = z/h$, for Model 1. Each of the three modes corresponds to the same wavenumber $\alpha = k_x h = 2$. The amplitudes for each mode correspond to the actual values of the displacements at $t = 0$. With reference to Eq. (3.25), $\xi = A_0 \tilde{q}_{k_0}$.

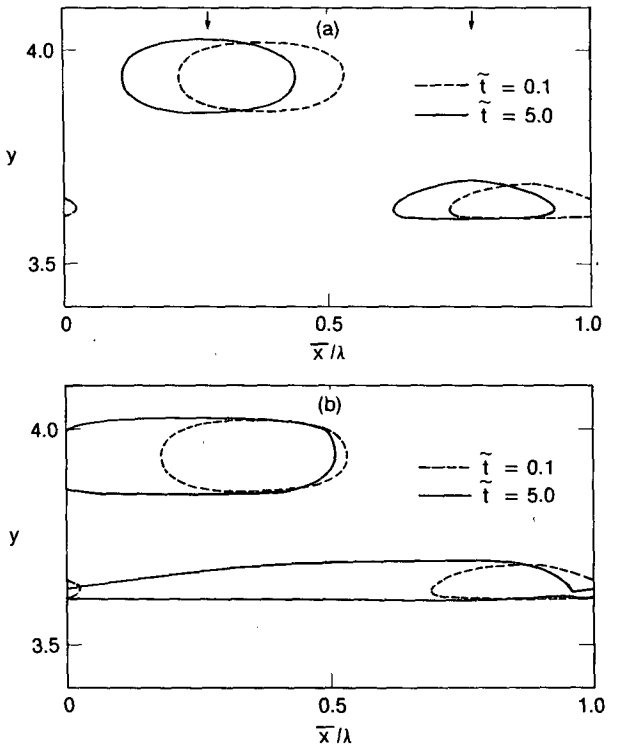

FIG. 4. (a) Regions within which the Richardson number is <¼, at a given time, for $n = 1$, and $\alpha = 2$ of Model 1. The horizontal coordinate is the horizontal distance (normalized with respect to the horizontal wavelength $\lambda = 2\pi/k_0$) measured in a frame of reference moving with the horizontal phase velocity of the wave. $\tilde{t} = tV/h$, where t is real time. Arrows indicate the values of $\bar{x}/\lambda$ corresponding to the maximum positive (left arrow) and negative vertical displacements. (b) As in (a), except for regions within which K is different from zero.

The appearance of regions with Ri less than zero needs very careful consideration. The linearized theory can produce such values where a more accurate non-linear treatment might leave Ri positive. It may also be inconsistent with the basic linearization to have points at which Ri is no longer positive. In many parameterizations, considerable importance is associated with the appearance of statically unstable regions, where relatively great increases in turbulent activity are presumed to occur. We have not followed this path, but have been very conservative, and retained only the weak parameterization characterizing Ri > 0. The more dramatic non-linear couplings involving convective overturning, while clearly of great interest, are beyond the scope of this investigation.

Further support for the interaction described here can be sought in the values of K obtained in the calculations. For $\tilde{t} = 0.1$ the maximum value of K is ~ 4 m^2 s^{-1}, while for $\tilde{t} = 5$ it is ~ 40 m^2 s^{-1}. If one considers the fact that these values are peak values and not time or spatial averages, one recognizes that they are well within the expected values for a stably stratified boundary layer (Brost and Wyngaard, 1978; Finnigan and Einaudi, 1981). Similar results for Model 2 are presented in Fig. 8.

Finally, the modulus and the phase of $A(t)$ are plotted in Figs. 5 and 9, for Models 1 and 2, respectively. Although the two models have very different temperature and velocity distributions, the general behavior of both sets of curves is quite similar, so they will be discussed together. $A(t)$ grows as a function of time with a logarithmic growth, which for the normalized time $\tilde{t} \approx 5$ ranges from ~ 0.004 s^{-1} for Model 1 to ~ 0.001 s^{-1} for $n = 0$ of Model 2. For smaller values of $\tilde{t}$, even larger values of the logarithmic growth are evident. These growth rates are quite respectable and well within the range encountered in the Kelvin–Helmholtz type of shear instability, with the same spatial and velocity scales. It appears, then, that such a wave-turbulence interaction is, at least initially, an effective mechanism for transferring energy into the wave.

The phase of the wave varies with time and thus reduces somewhat the effectiveness of the feedback mechanism: such effectiveness would be maximum if the phase were zero.

In Fig. 5 we have also drawn a dot-dot-dash line which corresponds to having set $K = K_0 = \bar{K}$. In this case, the phase of $A(t)$ is equal to 180° and therefore

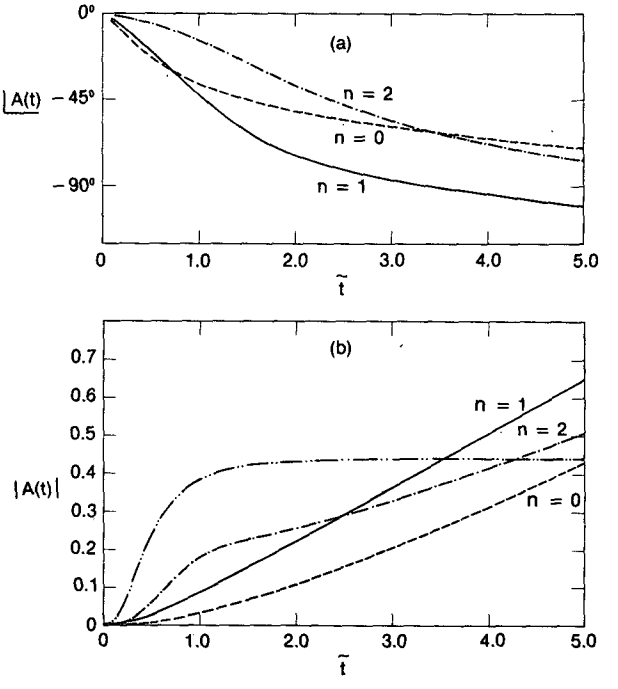

FIG. 5. Plots of the phase and amplitude of the function $A(t)$ versus normalized time $\tilde{t} = tV/h$, for $\alpha = 2$ and for modes $n = 0$, 1 and 2 of Model 1. The dot-dot-dash line corresponds to the case $n = 1$, $\alpha = 2$ in which we have set $K = \bar{K}$: for such a case the phase of $A(t)$ is constant and equal to 180°. $A(t)$ is defined by (3.25) and (3.26).

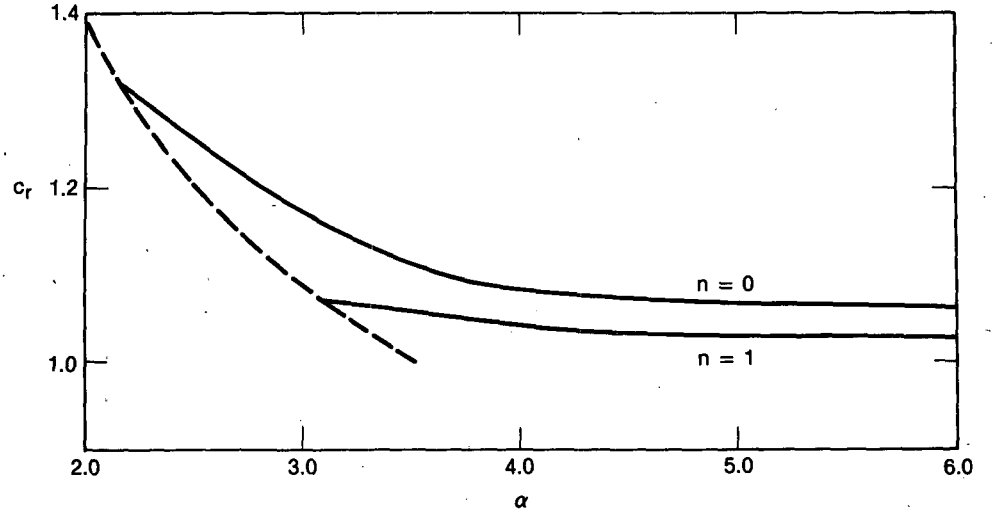

FIG. 6. As in Fig. 2, except for Model 2. The dotted line limits to the left the possible nonsingular neutral modes of our system.

$A(t)$ forces the wave to decay: the turbulent stresses are in phase with the strain rate $\mathbf{S}_{ij}$ and the turbulence absorbs energy from the wave. The dot-dash line of Fig. 9 has the same meaning. It follows then that in the cases we have presented here, the wave-dependent perturbation of the eddy coefficient K_1 is strong enough and in the right phase relation with the wave to overcome the effect of K_0 and, in fact, reverse the sign of the interaction. Where the feedback is negative, the effect of K_0 turns out to be dominant. We have indeed observed such cases for both models without, however, being able to establish any discernible pattern in the (α, c_r) parameter space.

5. Conclusions

We have presented analytical and numerical calculations describing the interaction of a monochromatic wave with a turbulence induced by the wave itself. The initial background temperature and wind profiles are such that the Richardson number is everywhere larger than ¼, although over some height ranges it is close to ¼. A neutral gravity wave, propagating through such a system, lowers the Richardson number below ¼ and triggers the formation of turbulence. The turbulence is modeled with a "1½th order" scheme which allows us to calculate the Fourier representation, at each height and time step, of the eddy diffusion coefficient. For certain regions of the spectrum, the fluctuating part of this coefficient overcomes the damping effect of the mean part, with the final result of the wave amplitude increasing in time. The growth rates involved are substantial, suggesting that a wave with small initial amplitude, which succeeds in triggering turbulence, may lead to a system with both wave and turbulence co-existing, each with substantial strength. The values we obtain for the eddy diffusion coefficients appear quite capable of producing the observed mixing rates above the surface layer.

The detailed mechanism through which the energy

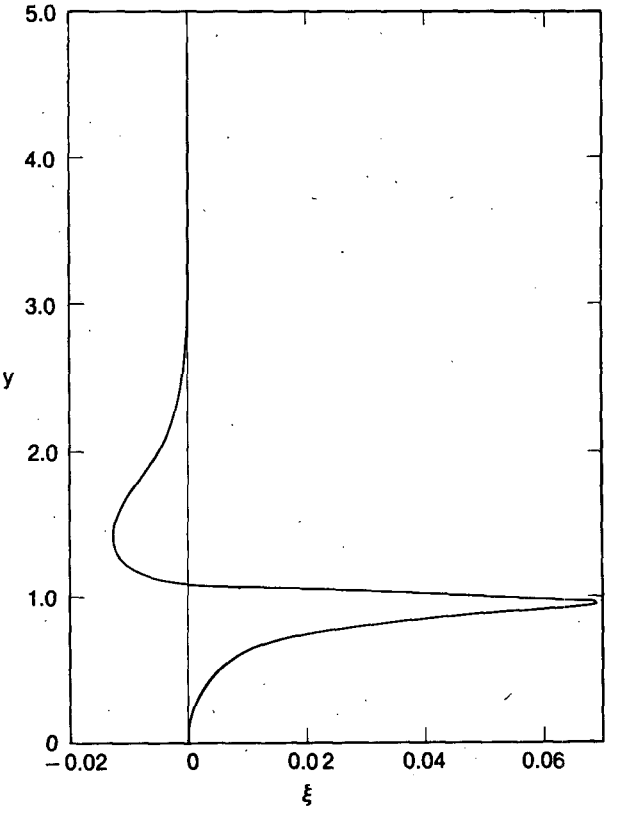

FIG. 7. As in Fig. 3, except for Model 2: $\alpha = 3.2$ and $n = 1$.

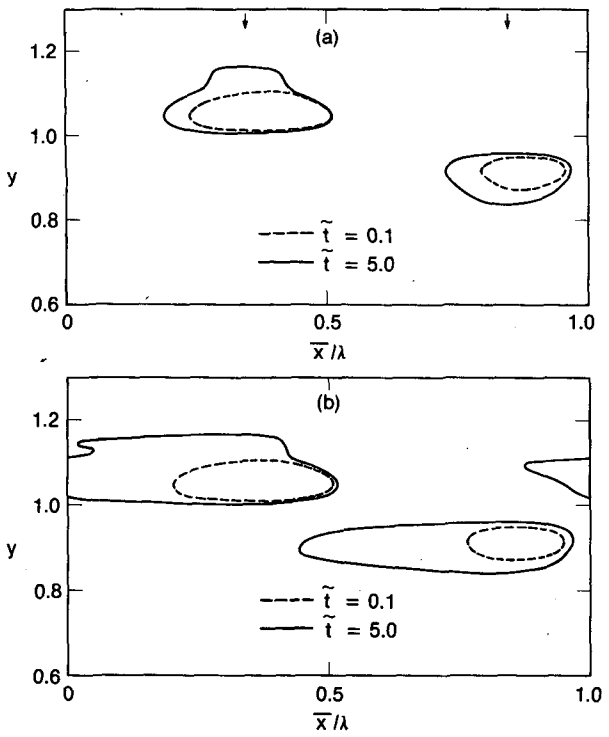

FIG. 8. As in Fig. 4, except for Model 2: $\alpha = 3.2$ and $n = 1$.

exchange takes place could be carried out through the analysis of the equation for the time evolution of the wave kinetic energy (Finnigan and Einaudi, 1981). One could then see that the sign of the energy exchange between the wave and the turbulence largely depends on the phase relationship between the wave-like stresses and the gradients of the wave field. Thus, fundamental to our model is the assumption discussed in Section 2, of the existence of a fluctuating part to the eddy diffusion coefficient K. The analysis of Finnigan and Einaudi (1981) and that which we are presently carrying out on new data from the Boulder Atmospheric Observatory suggests that indeed the $\tilde{r}_{ij}$'s and $\tilde{e}$'s have substantial harmonic content.

While we are fully aware that our results may depend on the assumed model for the turbulence, we believe that, within the assumed model, they do not depend on the chosen set of numerical parameters. Furthermore, they do not seem to be particularly sensitive to the initial amplitude of the wave or, conversely, to how close to ¼ the initial Richardson number Ri_0 is: this, of course, within the limits of the wave being linear and Ri_0 satisfying (3.1). Condition (3.1) is restrictive and the results presented here should not be extrapolated to cases of values of Ri_0 of order one, for example, or larger. Despite a number of numerical experiments within the adopted background temperature and wind profiles, we have not been able to determine a set of criteria which would allow us to predict which horizontal wavelength and period would produce a positive feedback. As one varies α along the $n = 1$ curve of Fig. 6, for example, ranges of negative feedback alternate with ranges of positive

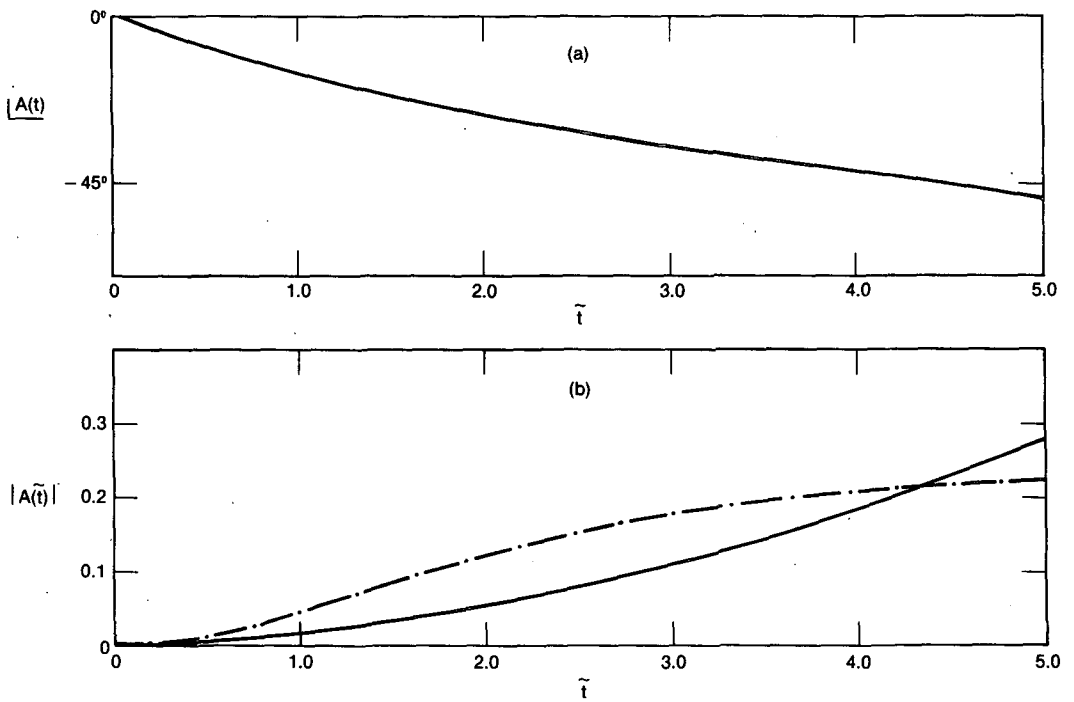

FIG. 9. As in Fig. 5, except for Model 2: $\alpha = 3.2$ and $n = 1$. The dot-dash line corresponds to the case $K = \tilde{K}$ for which the phase of $A(t)$ is 180°.

feedback, which we have not been able to interpret. This fact is perhaps not too surprising because the interaction depends in a complicated manner on the background state and on the vertical structure of the disturbance, with the latter often a sensitive function of ω and α.

Finally, we should point out again that our analysis only applies during the initial stages of the interaction. This is because we do not include in the system the effect of changes in the background state caused by the wave and the turbulence or any other nonlinear term which would further change the wave and the turbulence structure. As time evolves and the wave and the turbulence grow, one expects all the terms to become important.

Acknowledgments. We are grateful to Dr. J. J. Finnigan for many discussions of this subject. We would like to express our gratitude to the Wave Propagation Laboratory of NOAA for its support during the course of this work. D.F. was in receipt of a CIRES Visiting Fellowship during the first part of this study. F.E. and D.F. received partial support from NOAA grant number NA80RAD00013. Finally, parts of the numerical calculation were carried out at the National Center for Atmospheric Research, which is sponsored by the National Science Foundation; this support is gratefully acknowledged.

APPENDIX

Derivation of Eqs. (2.8) and (2.23).

Eqs. (2.8)–(2.10) are derived from the equivalent nonlinear set (2.1)–(2.3) in the following manner. Starting from Eq. (2.1) and using the decomposition (2.5), we can write Eq. (2.1) as

$$\bar{\rho}\Big[\frac{\partial}{\partial t}(\bar{u}_i+\tilde{u}_i+u_i')+(\bar{u}_j+\tilde{u}_j+u_j')\times\frac{\partial}{\partial x_j}(\bar{u}_i+\tilde{u}_i+u_i')\Big]=-\frac{\partial}{\partial x_i}(\bar{p}+\tilde{p}+p')-(\bar{\rho}+\tilde{\rho}+\rho')g\delta_{i3}\,. \quad \text{(A1)}$$

The variations of density in the inertial terms have been neglected. Taking the time and phase averages of (A1) we obtain two equations whose difference is given by

$$\bar{\rho}\Big[\frac{\partial}{\partial t}\tilde{u}_i+\bar{u}_j\frac{\partial}{\partial x_j}\tilde{u}_i+\tilde{u}_j\frac{\partial}{\partial x_j}\bar{u}_i\Big]=-\frac{\partial\tilde{p}}{\partial x_i}-g\tilde{\rho}\delta_{i3}-\bar{\rho}\Big[\tilde{u}_j\frac{\partial}{\partial x_j}\tilde{u}_i-\overline{\tilde{u}_j\frac{\partial}{\partial x_j}\tilde{u}_i}\Big]-\bar{\rho}\Big[\langle u_j'\frac{\partial}{\partial x_j}u_i'\rangle-u_j'\frac{\partial}{\partial x_j}u_i'\Big]. \quad \text{(A2)}$$

Eq. (2.8) follows from (A2), if the continuity Eq. (2.2) is simplified to give

$$\nabla\cdot(\bar{\rho}\tilde{u}_i)=0,\quad \nabla\cdot(\bar{\rho}u_i')=0. \quad \text{(A3)}$$

Subtracting from (A1) its own phase average, multiplying by u_i' and phase averaging, we obtain the equation for the kinetic energy of the turbulent fluctuations:

$$\frac{\partial}{\partial t}v^2+(\bar{u}_j+\tilde{u}_j)\frac{\partial}{\partial x_j}v^2=-\langle u_j'\frac{\partial}{\partial x_j}\frac{1}{2}u_i'u_i'\rangle-\langle u_i'u_j'\rangle\frac{\partial}{\partial x_j}(\bar{u}_i+\tilde{u}_i)-\frac{1}{\bar{\rho}}\langle u_i'\frac{\partial}{\partial x_i}p'\rangle+g\langle u_i'\Theta'\rangle\delta_{i3}/(\bar{\Theta}+\tilde{\Theta})+\nu\Big[\frac{\partial^2v^2}{\partial x_j\partial x_j}-\Big\langle\Big(\frac{\partial u_i'}{\partial x_j}\Big)^2\Big\rangle\Big], \quad \text{(A4)}$$

where v^2 is defined by (2.24). Here the viscous term involving the kinematic viscosity ν was reintroduced, since the turbulence involves scales at which viscous effects are important. The next to the last term on the right-hand side of (A4) corresponds to the usual approximation in turbulence theory of replacing the turbulence fluctuations of density with those of potential temperature. Using (2.13) and neglecting the triple products, the pressure term (Monin and Yaglom, 1971) and the viscous diffusion term (A4) reduces to (see also Zeman, 1981):

$$\frac{\partial}{\partial t}v^2+(\bar{u}_j+\tilde{u}_j)\frac{\partial}{\partial x_j}v^2=-(\tfrac{2}{3}v^2\delta_{ij}-K\mathbf{S}_{ij})\frac{\partial}{\partial x_j}(\bar{u}_i+\tilde{u}_i)+g\langle u_i'\Theta'\rangle\delta_{i3}/(\bar{\Theta}+\tilde{\Theta})-\epsilon_d\,, \quad \text{(A5)}$$

where ϵ_d represents the rate of turbulence energy dissipation. Finally, using the approximation (2.25) in (A5), Eq. (2.23) is obtained.

REFERENCES

Batchelor, G. K., 1953: *The Theory of Homogeneous Turbulence.* Cambridge University Press, 197 pp.

Brost, R. A., and J. C. Wyngaard, 1978: A model study of the stably stratified planetary boundary layer. *J. Atmos. Sci.*, **35**, 1427–1440.

Browning, K. A., and C. D. Watkins, 1970: Observations of CAT by high power radar. *Nature*, **227**, 260–263.

——, ——, J. R. Starr and A. McPherson, 1970: Simultaneous measurements of CAT at the tropopause by high-power radar and instrumented aircraft. *Nature*, **228**, 1065–1067.

Chimonas, G., 1972: The stability of a coupled wave-turbulence system in a parallel shear flow. *Bound.-Layer Meteor.*, **2**, 444–452.

——, F. Einaudi and D. P. Lalas, 1980: A wave theory for the onset and initial growth of condensation in the atmosphere. *J. Atmos. Sci.*, **37**, 827–845.

Courant, R., and D. Hilbert, 1953: *Methods of Mathematical Physics*, Vol. 1. Interscience, 560 pp.

Deardorff, J. W., 1973: The use of subgrid transport equations in a three-dimensional model of atmospheric turbulence. *J. Fluids Eng.*, **95**, 429–438.

——, 1974: Three dimensional numerical study of the height and mean structure of a heated planetary boundary layer. *Bound.-Layer Meteor.*, **7**, 81–106.

Finnigan, J. J., and F. Einaudi, 1981: The interaction between an internal gravity wave and the planetary boundary layer. Part II: The effect of the wave on the turbulence structure. *Quart. J. Roy. Meteor. Soc.*, **107**, 807–832.

Gossard, E. E., D. R. Jensen and J. H. Richter, 1971: An analytical study of troposphere structure as seen by high-resolution radar. *J. Atmos. Sci.*, **28**, 794–807.

Hodges, R. R., Jr., 1967: Generation of turbulence in the upper atmosphere by internal gravity waves. *J. Geophys. Res.*, **72**, 3455–3458.

——, 1969: Eddy diffusion coefficients due to instabilities in internal gravity waves. *J. Geophys. Res.*, **74**, 4087–4090.

Kondo, J., O. Kanechika and N. Yasuda, 1978: Heat and momentum transfers under strong stability in the atmospheric surface layer. *J. Atmos. Sci.*, **35**, 1012–1021.

Lumley, J. L., and H. A. Panofsky, 1964: *The Structure of Atmospheric Turbulence*. Interscience, 239 pp.

Monin, A. S., and A. M. Yaglom, 1971: *Statistical Fluid Mechanics: Mechanics of Turbulence*, Vol. I. MIT Press, 769 pp.

Morse, P. M., and H. Feshbach, 1953: *Methods of Theoretical Physics*, Part 1. McGraw Hill, 997 pp.

Orlanski, I., and K. Bryan, 1969: Formation of the thermocline step structure by large amplitude internal gravity waves. *J. Geophys. Res.*, **74**, 6975–6983.

——, and C. P. Cerasoli, 1981: Energy transfer among internal gravity modes: weak and strong interactions. *J. Geophys. Res.*, **86**, 4103–4124.

Phillips, O. M., 1980: *The Dynamics of the Upper Ocean*. Cambridge University Press, 336 pp.

Reynolds, W. C., and A. K. M. F. Hussain, 1972: The mechanics of an organized wave in turbulent shear flow. Part 3. Theoretical models and comparisons with experiments. *J. Fluid Mech.*, **54**, 263–288.

Van Zandt, T. E., J. L. Green, K. S. Gage and W. L. Clark, 1978: Vertical profiles of refractivity turbulence structure constant: Comparison of observations by the Sunset radar with a new theoretical model. *Radio Sci.*, **13**, 819–829.

Yamada, T., and G. L. Mellor, 1979: A numerical simulation of BOMEX data using a turbulence closure model coupled with ensemble cloud relation. *Quart. J. Roy. Meteor. Soc.*, **105**, 915–944.

Zeman, O., and J. L. Lumley, 1976: Modeling buoyancy driven mixed layers. *J. Atmos. Sci.*, **33**, 1974–1988.

——, 1981: Progress in the modeling of planetary boundary layers. *Annual Review of Fluid Mechanics*, Vol. 13, Annual Reviews, Inc., 253–272.